Bulletin of the National Research Centre

RESEARCH

Open Access

Analysis of chemical, ion slip, and thermal radiation effects on an unsteady magnetohydrodynamic dusty fluid flow with heat and mass transfer through a porous media between parallel plates

Wael Abbas[1], Osama Khaled[2], Salah Beshir[2], Mostafa Abdeen[2] and Mohamed Elshabrawy[2,3*]

Abstract

Background Investigating the dusty fluids flow attracted substantial attention in latest years because of their widespread utility within several industrial applications, including polymer technology, gas cooling systems, combustion, petroleum industry, and transport processes. The current article is dedicated to inspect the flow with mass transfer and heat of an unsteady Magneto-hydrodynamic dusty fluid. Consequently, impacts of chemical and thermal radiation, Joule, ion slip, Hall, and viscous dissipation toward heat and mass transferring and fluid flows are provided.

Results Numerical solution of the controlling partial differential equations was performed. The temperature, velocity, and distribution of concentration for the particle and fluid phases were inspected under the influences of various physical parameters and their discussion was supplemented with diagrams.

Conclusions The findings specify that these parameters have a significantly governed the solutions. The thermal radiation denotes efficiency enhancement of temperature distribution.

Keywords Dusty fluid, Heat and mass transfer, Couette flow, Chemical reaction, Thermal radiation

Background

The dusty fluids' heat transfer and flow studies are extremely useful in improving the operation of many applications in several industries and engineering problems, including dust collection, atmospheric fallout, powder technology, nuclear reactor, and paint spraying (Islam et al. 2022). The dusty fluid flow under the simplifying assumptions was formulated by (Saffman 1962). Hence, development and research are used to enhance the flow and heat transfer of dusty fluids attributes by using various models and situations have been previously documented (Michael and Miller 1966; Peddieson 1976; Meena et al. 2022; Safwa et al. 2022; Dey and Chutia 2022, Tavousi et al. 2023). Recently, many investigators studied the flows of particle fluids under different conditions are carried out. Attia et al. (2014) examined the fluid flow of the unsteady dusty with heat transfer in the existence of uniform injection and suction and porosity impact through parallel plates. The mathematical solutions for dual-phase dusty boundary-layer non-Newtonian fluid

*Correspondence:
Mohamed Elshabrawy
mmshabrawy@nu.edu.eg
[1] Basic and Applied Science Department, College of Engineering and Technology, Arab Academy for Science, Technology, and Maritime Transport, Cairo, Egypt
[2] Engineering Mathematics and Physics Department, Faculty of Engineering, Cairo University, Giza, Egypt
[3] Smart Engineering Systems Research Center (SESC), Nile University, Sheikh Zayed City, Egypt

flow through the semi-infinite vertical heated surface are obtained (Hamid et al. 2022). Mahanthesh et al. (2019a, b) investigated the nonlinear convective transport influence on non-Newtonian Dusty fluids flow through a stretched sheet. The influence of thermal radiation of squeezed dusty fluid flow with heat transfer between parallel plates was examined by Abbas et al. (2020). Chandrawat et al. (2022) inspected numerically the unsteady flow of two unmixable micropolar and dusty fluids throughout a horizontal plate. Several researchers were interested in latest developments regarding dusty nano-fluids flow under different categories and conditions are highlighted with many researchers (Mishra et al. 2022; Dey and Chutia 2020; Gireesha et al. 2018). Several researchers have considered magnetohydrodynamics (MHD) flow of Newtonian/non-Newtonian fluids due to its substantial potentiality in scientific and industrial concerns (Jha and Apere 2013; Dey and Chutia 2020; Rafiq et al. 2022) The Hall influences are significant for the MHD applications. It is toward the conducting fluid is an ionized gas with and strong magnetic field (Abbas and Sayed 2017). Because the reduction in conductivity is normal to the magnetic field as a result of the electrons and ions free spiraling about the force's magnetic lines before collisions and a current is stimulated normal to both magnetic and electric fields. Bafakeeh et al. (2022) examined the Hall influences regarding the hydromagnetic oscillatory unsteady flow for non-Newtonian second-grade fluid. The analytical solution for an unsteady dusty fluid flow throughout a circular pipe having an Ion Slip effect was studied by Abdeen et al. (2013). Alkot and Abbas (2017) reported the mathematical procedure of blood flow throughout catheterized arteries having overlapping stenosis under the hall effect. The exponential heat source and hall effects on unsteady dusty nanofluid with time-dependent velocity were studied in Hussein (2023), Mahanthesh et al. (2019a, b). The impact of chemical reactions has very important because it has many industrial applications in chemical engineering, food processing, oil emulsions, and geothermal reservoirs.

Muthuraj et al. (2016) inspected the peristaltic motion of dusty fluid having mass transfer and heat through a horizontally straight channel under a chemical reaction effect. The MHD stagnation point of nanofluid Casson flow with heat transfer toward a stretched sheet under activation energy and chemical reaction effect was investigated (Khan et al. 2018). Kumar et al. (2021) explored the chemical reaction and heat source impact on the MHD flow of the blood in bifurcated permeable arteries. The chemical reaction influence on the peristaltic electroosmotic flow of Jeffrey nanofluid was investigated in the existence of the Brownian effect (Rafiq et al. 2022). Also, there are numerous researchers who investigated the problems pf the dusty flow by considering the effect of thermal radiation (Abo-zaid et al. 2021; Mahanthesh et al. 2021; Ghadikolaei et al. 2018; Rafiq et al. 2022).

In the current study, we are motivated to examine the flow with mass transfer and heat of an unsteady MHD dusty fluid under thermal radiation and chemical reaction effects. Viscous dissipation and Joule, ion slip, Hall, and heat generation is considered. The controlling nonlinear equations for the particles and fluid are solved mathematically by the finite difference technique. The influences of suitable non-dimensional parameters on the temperature, concentration, and velocity profiles are considered and analyzed with the assistance of diagrams.

The dusty fluid flow throughout horizontal porous plates was considered. Figure 1 shows a diagram of physical geometry. While the lower plate is immobile, the upper one moves in the x-direction with an unvarying velocity $\mathbf{u}_{\boldsymbol{o}}$. A uniform injection and suction through the plates are considered in the y-direction with constant velocity vo. Both plates are regarded as non-conductive electrically and preserved within two fixed temperatures and the species concentration.

At the lower wall $\mathbf{T}_{\boldsymbol{o}}$,$\mathbf{C}_{\boldsymbol{o}}$, $\mathbf{T}_1$ and $\mathbf{C}_1$ for the upper wall where $\mathbf{T}_1 > \mathbf{T}_{\boldsymbol{o}}$. In this study, a uniform magnetic field with strength $\mathbf{B} = (0, 0, \mathbf{B}_{\boldsymbol{o}})$ is applied perpendicularly toward the plates (positive y-direction). Additionally, the lack of Hall current is related to the magnetic field incidence, which likely influences fluid flow motion. The thermal equation takes into account radiation, Joule and viscous dissipations, and heat generation are taken into account in the species equation. Additionally, the flow is assumed to be non-compressible, and the two phases have constant densities, and there exists a chemical reaction in the mixture.

According to the aforementioned assumptions the basics equations are (Abbas et al. 2020).

Fluid phase.

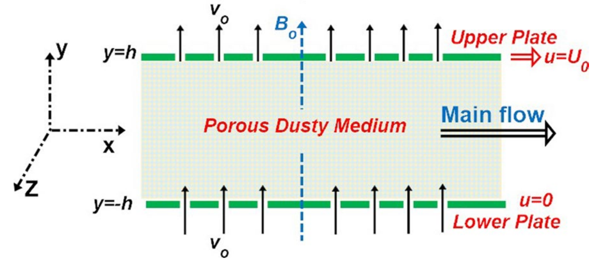

Fig. 1 Sketch of the problem

$$\rho \frac{D\mathbf{v}}{Dt} = -\nabla \mathbf{p} + \mu \nabla^2 \mathbf{v} + \mathbf{J} \times \mathbf{B} - KN(\mathbf{v} - \mathbf{v}_{\boldsymbol{p}} - \frac{\mu}{K_D}\mathbf{v} \tag{1}$$

$$c_p \frac{D\mathbf{T}}{Dt} = k_f \nabla^2 \mathrm{T} + \frac{\mathbf{J}.\mathbf{J}}{\boldsymbol{\sigma_f}} - \frac{1}{\gamma_T}\left(\mathrm{T}_p - T\right) + \varphi + \nabla .q_r + Q(T - T_o) \tag{2}$$

$$\frac{D\mathbf{C}}{Dt} = D_B \nabla^2 \mathrm{C} + k_c (C - C_o) \tag{3}$$

Particle phase:

$$\rho_p \frac{D\boldsymbol{v_p}}{Dt} = \mathrm{KN}(\mathbf{v} - \mathbf{v_p}) \tag{4}$$

$$\frac{D\boldsymbol{T_p}}{Dt} = \frac{1}{\gamma_T}\left(T_p - T\right) \tag{5}$$

where ρ, ρ_p are the fluid and particles densities, v denotes the fluid velocity vector, $\mathbf{v} = u(y,t)\boldsymbol{i} + vo\boldsymbol{j} + w(y,t)\boldsymbol{k}$, $\mathbf{p}$ the pressure gradient, μ denotes fluid viscosity. $KN\left(v - v_p\right)$ is the force resulted from the relative motion among dust particles and fluid, whereas K represents the Stoke's drag constant which is $\mathrm{K} = 6\pi\mu\mathrm{ra}$ in case of spherical particles having radius a, N denotes the dust particles' number density per unit volume of the fluid, v_p is the dust particles' velocity vector, and K_D is the Darcy permeability. T denotes the fluid temperature, T_p is the dust temperature, c_p denotes the fluid specific heat capacity at fixed volume, k_f denotes the fluid thermal conductivity, γ_T denotes the temperature relaxation time, and c_s denotes the particles specific heat capacity. φ represents the viscous dissipation, q_r denotes the radiative heat flux, and Q is heat source constant. C denotes the concentration, D_B denotes the diffusion coefficient, and k_c is the chemical reaction parameter. $\mathbf{J}$ accounts for the current density, and $\mathbf{B}$ accounts for total magnetic induction vector. When the ion slip and Hall terms are maintained, the current density $\mathbf{J}$ from the general Ohm's law can be obtained by Attia et al. (2015):

$$\mathbf{J} = \sigma\left[\mathbf{v} \times \mathbf{B} - \beta(\mathbf{J} \times \mathbf{B}) + \frac{\beta B_i}{B_o}(\mathbf{J} \times \mathbf{B}) \times \mathbf{B}\right] \tag{6}$$

where σ represents the electric conductivity and $B_i$and β denote the ion slip parameter and Hall factor. Lorentz force can be represented as

$$\mathbf{J} \times \mathbf{B} = \frac{\sigma B_o^2}{(1 + \mathrm{Bi\ Be})^2 + \mathrm{Be}^2}((1 + \mathrm{Bi\ Be})u + \mathrm{Be}w)\mathbf{i} + ((1 + \mathrm{Bi\ Be})w - \mathrm{Be}u)\mathbf{k} \tag{7}$$

where $\mathrm{Be} = \sigma\beta B_o$ denotes the Hall parameter. The heat flux according to the Rosseland approximation is manifested by:

$$q_r = -\frac{4\sigma^*}{3k^*}\frac{\partial T^4}{\partial y} \tag{8}$$

where σ∗and k∗account for the Stefan–Boltzmann constant and the mean absorption coefficient, respectively. Furthermore, T^4 could be written using the Taylor series about T_o as:

$$T^4 \cong 4T_o^3 T - 3T_o^4 \tag{9}$$

By substituting Eqs. (6–9) into Eqs. (1–5) and after some arrangements yield:

Fluid phase:

$$\rho\left(\frac{\partial u}{\partial t} + v_o\frac{\partial u}{\partial y}\right) = -\frac{dp}{dx} + \mu\frac{\partial^2 u}{\partial y^2} - \frac{\sigma B_o^2}{(1 + \mathrm{Bi\ Be})^2 + \mathrm{Be}^2}((1 + \mathrm{Bi\ Be})u + \mathrm{Be}w) - KN\left(u - u_p\right) - \frac{\mu}{K_D}u \tag{10}$$

$$\frac{\partial w}{\partial t} + \rho v_o\frac{\partial w}{\partial y} = \mu\frac{\partial^2 w}{\partial y^2} - \frac{\sigma B_o^2}{(1 + \mathrm{Bi\ Be})^2 + \mathrm{Be}^2}((1 + \mathrm{Bi\ Be})w - \mathrm{Be}u) - KN\left(w - w_p\right) - \frac{\mu}{K_D}\mathrm{w} \tag{11}$$

$$\rho c\frac{\partial T}{\partial t} + \rho c v_o\frac{\partial T}{\partial y} = k_f\frac{\partial^2 T}{\partial y^2} + \mu\left(\left(\frac{\partial u}{\partial y}\right)^2 + \left(\frac{\partial w}{\partial y}\right)^2\right) \frac{\sigma(1 + \mathrm{Bi\ Be})B_o^2}{(1 + \mathrm{Bi\ Be})^2 + Be^2}\left(u^2 + w^2\right) + \frac{\rho_p c_s}{\gamma_T}\left(T_p - T\right) + \frac{16\sigma^* T_o^3}{3\alpha^*}\frac{\partial^2 T}{\partial y^2} + Q\left(T_p - T\right) \tag{12}$$

$$\frac{\partial \mathrm{C}}{\partial t} + v_o\frac{\partial C}{\partial y} = D_B\frac{\partial^2 C}{\partial y^2} + k_c(C - C_o) \tag{13}$$

pick the following proper dimensionless forms

$$(\hat{x}, \hat{y}) = \frac{(x, y)}{h}, \quad \hat{t} = \frac{tU_o}{h},$$
$$(\hat{u}, \hat{w}) = \frac{(u, w)}{U_o}, \quad (\hat{u}_p, \hat{w}_p) = \frac{(u_p, w_p)}{U_o}$$
$$\hat{P} = \frac{P}{\rho U_o^2}, \quad \hat{T} = \frac{T - T_o}{T_1 - T_o},$$
$$\hat{T}_p = \frac{T_p - T_o}{T_1 - T_o}, \quad \hat{\Gamma} = \frac{C - C_o}{C_1 - C_o}$$

The non-dimensional forms after dropping the hats are:
Particle phase

$$m_p \frac{\partial u_p}{\partial t} = KN(u - u_p) \tag{14}$$

$$m_p \frac{\partial w_p}{\partial t} = KN(w - w_p) \tag{15}$$

$$\frac{\partial T_p}{\partial t} = -\frac{1}{\gamma_T}(T_p - T) \tag{16}$$

where m_p accounts for the dust particles' average mass. The initial and boundary conditions can be obtained by:
At $t \leq 0$:

$$u = u_p = w = w_p = 0; \quad T = T_p = T_o; \quad C = C_o$$

At $t > 0$:

$$u = u_p = w = w_p = 0;\ T = T_p = T_o; \quad C = C_o at y = -h$$

At $t > 0$:

$$u = u_p = U_0; \quad w = w_p = 0; \quad T = T_p = T_1; \quad C = C_1 \quad \text{at} \quad y = h \tag{17}$$

Fluid phase:

$$\frac{\partial u}{\partial t} + S\frac{\partial u}{\partial y} = -\frac{dP}{dx} + \frac{1}{Re\frac{\partial^2 u}{\partial y^2}\frac{H_a^2}{Re((1+BiBe)^2+Be^2)}\frac{R}{Re_p}} \tag{18}$$

$$\frac{\partial w}{\partial t} + S\frac{\partial w}{\partial y} = \frac{1}{Re\frac{\partial^2 w}{\partial y^2}\frac{H_a^2}{Re((1+BiBe)^2+Be^2)}\frac{R}{Re_p}} \tag{19}$$

$$\frac{\partial T}{\partial t} + S\frac{\partial T}{\partial y} = \frac{1}{\mathrm{RePr}}\frac{\partial^2 T}{\partial y^2} + \frac{E_c}{\mathrm{Re}}\left(\left(\frac{\partial u}{\partial y}\right)^2 + \left(\frac{\partial w}{\partial y}\right)^2\right) + \frac{(1+BiBe)H_a^2 E_c}{\mathrm{Re}\left((1+BiBe)^2 + Be^2\right)}\left(u^2 + w^2\right) + \frac{2R}{3\mathrm{Pr}}\left(T_p - T\right) + Q_s\hat{T} + Q_r\frac{\partial^2 T}{\partial y^2} \tag{20}$$

$$\frac{\partial \Gamma}{\partial t} + S\frac{\partial \Gamma}{\partial y} = \frac{1}{S_C}\frac{\partial^2 \Gamma}{\partial y^2} + \gamma_C\Gamma \tag{21}$$

Particle phase:

$$G\frac{\partial u_p}{\partial t} = u - u_p \tag{22}$$

$$G\frac{\partial w_p}{\partial t} = w - w_p \tag{23}$$

$$\frac{\partial T_p}{\partial t} = -L_o(T_p - T) \tag{24}$$

where $R_e = \rho U_0 h/\mu$ is the Reynolds number, $Ha^2 = \sigma B_0^2 h^2/\mu$ denotes the Hartmann number squared, $S = v_0/U_0$ denotes the suction parameter, $E_c = {U_0}^2/C_p(T_2 - T_1)$ is the Eckert number, $G = m_p\mu/\rho h^2 K$, denotes the particle mass parameter, $R = KNh^2/\mu$ denotes the concentration parameter, $L_o = \rho h^2/\mu\gamma_T$ denotes the temperature relaxation time parameter, $Q_s = hQ/\rho c u_o$ is the heat source parameter and $Q_r = -16\sigma^* T_o^3/3\rho c u_o$ is the radiation parameter, $\gamma_c = hk_c/u_o$ is the chemical reaction parameter, and $M = h\mu/\rho u_o k_D$ is the porous medium parameter.

The dimensionless initial and boundary conditions are:
At $t \leq 0$:

$$u = u_p = w = w_p = 0; \quad T = T_p = 0; \quad \Gamma = 0$$

At $t > 0$:

$$u = u_p = w = w_p = 0; \quad T = T_p = 0; \quad \Gamma = 0 \quad \text{at} \quad y = -1$$

At $t > 0$:

$$u = u_p = 1; \quad w = w_p = 0; \quad T = T_p = 1; \quad \Gamma = 1 \quad \text{at} \quad y = 1 \tag{25}$$

Methods

The system of governing partial differential Eqs. (18)–(24) with the corresponding boundary conditions (25) are increasingly nonlinear and coupled, consequently, the precise solution cannot be found. Therefore, the mathematical solution to these equations can be obtained through the finite difference technique. The Crank-Nicolson implicit approach is employed and is accomplished via applying an average of the schemes of central divided difference at successive time points. The main definition and procedure of this technique were formerly presented in several research (Abdeen et al. 2013; Alkot and Abbas 2017).

Results

The physical quantities for engineering interest, the local skin friction (τ), local Nusselt number (Nu), and local Sherwood number (Sh) are defined as (Pandya et al. 2017):

- skin friction coefficient: $\tau = \left(\frac{\partial u}{\partial y}\right)_{y=0}$
- Nusselt number: $Nu = -\left(\frac{\partial T}{\partial y}\right)_{y=0}$
- Sherwood number: $Sh = -\left(\frac{\partial C}{\partial y}\right)_{y=0}$

To validate the accuracy of presented results and methodology, the current results are compared with the previously published available results in some special cases, which was reported by Pandya et al. (2017). We recorded the compared values that skin friction coefficient values, Nusselt number and Sherwood number for various values of some parameters impact, which are illustrated in Tables 1 and 2. Generally, it is clear that, from this comparison the results are in excellent agreement.

The current study was conducted to investigate the flow with mass transfer and heat of an unsteady MHD dusty fluid under thermal radiation, viscous dissipation, Joule, chemical, and ion slip influences between parallel plates.

The finite differences technique was adopted for acquiring the fluid/dust particles' temperature, concentration, and velocity as a function of some physical aspects. The graphical outcomes are demonstrated at Figs. 2, 3, 4, 5, 6, 7, 8, 9, 10, and 11. Calculations were accomplished for $C = -5$, $R = 0.5$, $\mathrm{Re} = 1$, $\mathrm{Lo} = 0.7$, $G = 0.8$, $P_r = 1$.

Discussion

The time variation profiles against the fluid/dust main velocities components u, u_p, secondary velocities components w, w_p, and temperatures T, T_p, and fluid concentration Γ, respectively, are depicted in Figs. 2, 3, 4, and 5 for $\mathrm{Bi} = 3$, $\mathrm{Be} = 3$, $\mathrm{Ha} = 1$, $M = 1$, $S = 1$. In all these Figures, it is seen that the fluid/dust velocities, temperatures, and concentration increase with time till it reaches its steady state. It is found in Figs. 2, 3, and 4 that, the main velocities of dust and fluid attain steady state quicker relative to secondary velocities that attain it quicker than fluid temperature. It may be because of the fluid main velocity represents the source of the secondary velocity, and both are the sources of the fluid temperature. Moreover, it is seen that the fluid's temperature and velocity acquire steady state early relative to the particle phase that ascribes the fluid velocity as the source of the particle flow.

Figure 6 illustrates the particle and fluid temperature profiles for different thermal radiation values. It was observed that the temperature profiles are improved via rising the thermal radiation parameter values. However, Fig. 7 shows the fluid concentration progression with the time at the center of the channel ($y = 0$), for different chemical reaction parameter scores. It was recognized that the concentration is decreased by rising the chemical reaction parameter value. Figures 8, 9, 10, and 11 display the time progression of the fluid/dust temperature and main velocity profiles at $y = 0$, at different ion slip

Table 1 Comparison of Skin friction coefficient for various values of some parameters

γ_c	G	S_c	Q_r	R	τ	
					Present	Pandya et al. (2017)
1	1	1	2	1	− 0.47567	− 0.475593
1	1	1	2	1	1.02231	1.02161
3	1	1	2	1	0.424987	0.424903
5	1	1	2	1	0.30711	0.306442
7	1	1	2	1	− 0.17278	− 0.172543
1	0.1	0.6	2	1	0.916213	0.915588

Table 2 Comparison of Nusselt and Sherwood number for various values of some parameters

γ_c	G	S_c	Q_r	R	Nu		Sh	
					Present	Pandya et al. (2017)	Present	Pandya et al. (2017)
1	1	1	2	1	0.66527	0.665233	1.53678	1.53647
1	1	1	2	1	0.265673	0.265555	0.931123	0.930193
3	1	1	2	1	0.37676	0.37572	1.51134	1.51058
5	1	1	2	1	0.35824	0.358772	1.831231	1.83055
7	1	1	2	1	0.293456	0.292822	3.01123	3.00238
1	0.1	0.6	2	1	0.411678	0.411797	0.82992	0.82959

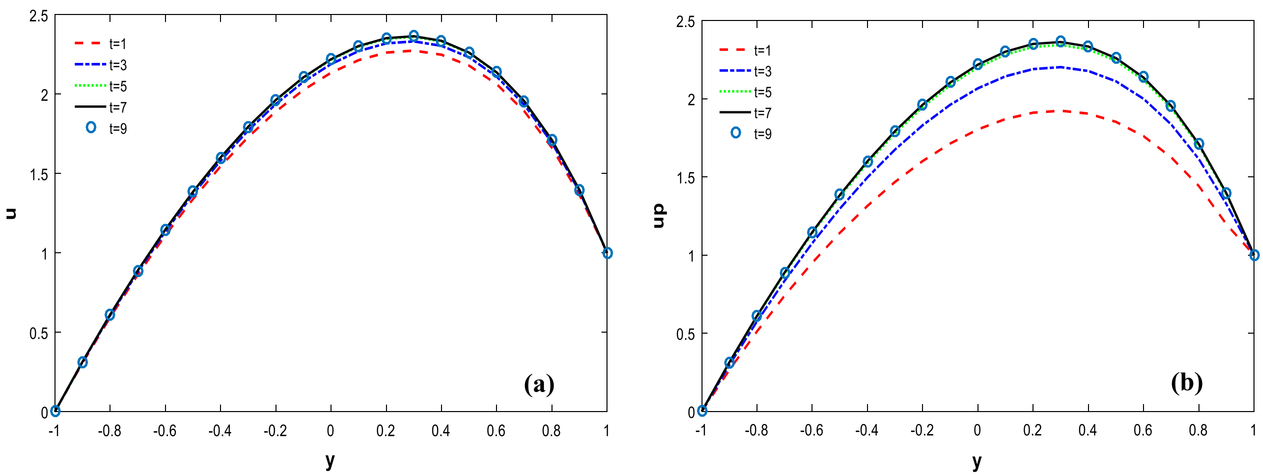

Fig. 2 Time variation against main velocity; **a** fluid velocity *u*; **b** dust velocity up

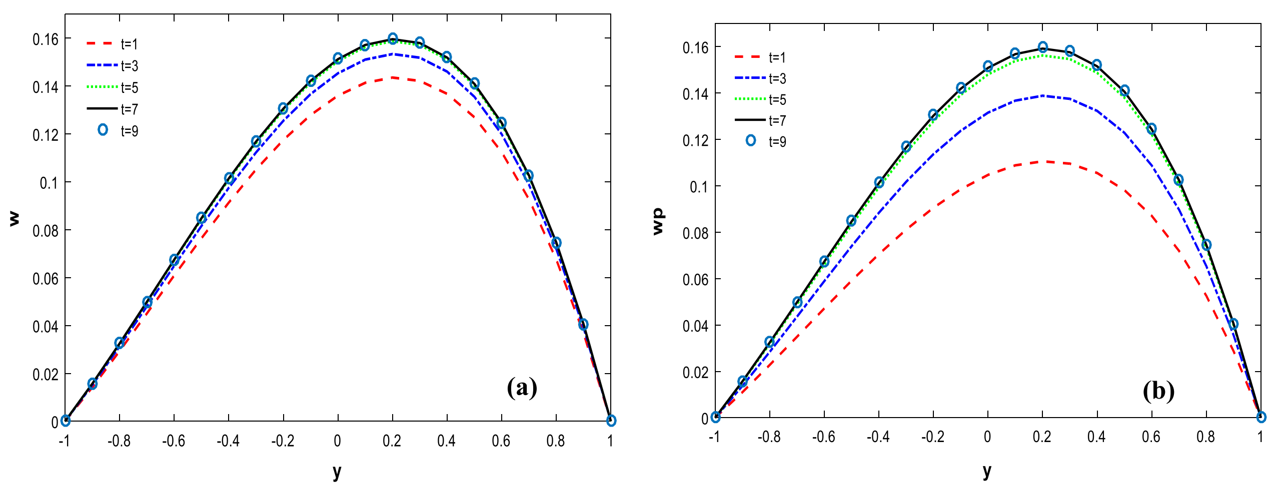

Fig. 3 Time variation against secondary velocity; **a** fluid velocity *w*; **b** dust velocity *wp*

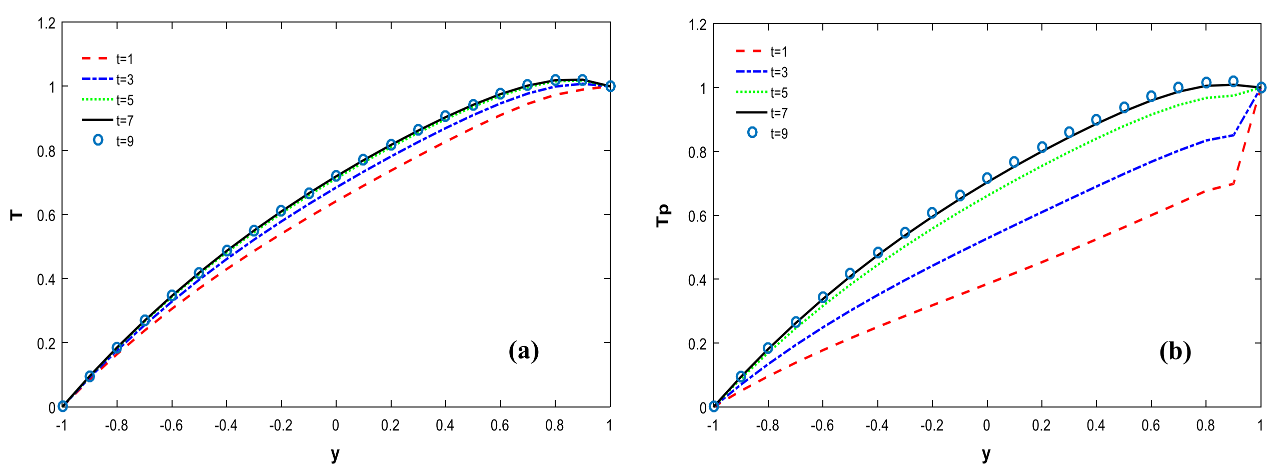

Fig. 4 Time variation against temperature; **a** fluid temperature T; **b** dust temperature T_P

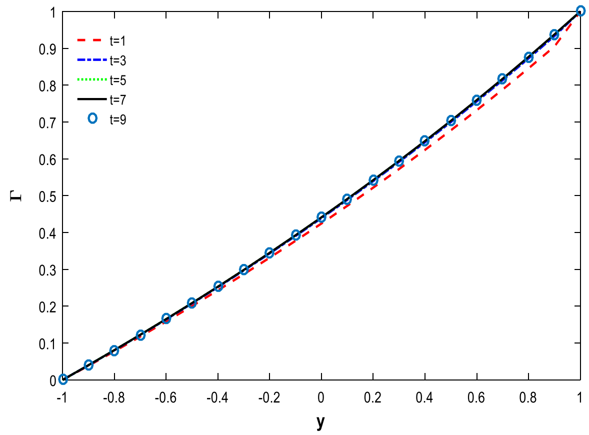

Fig. 5 Time variation against fluid Concentration Γ

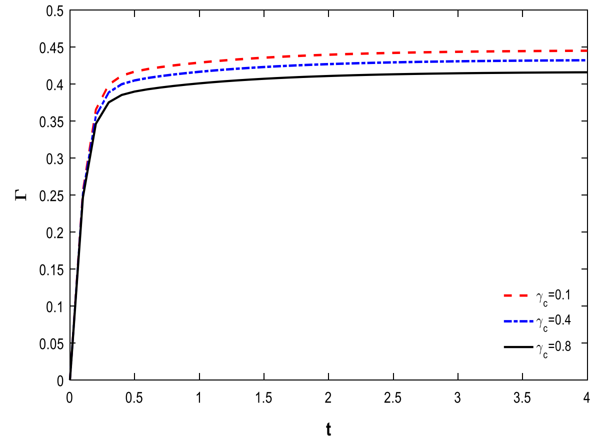

Fig. 7 Influence of γ_c on fluid concentration at channel center

and Hall parameters values. Figures 8 and 9 demonstrate the influence of Be and Bi parameters on the particle and fluid main velocity profiles. The particle and fluid main velocity profiles are recognized to increase with increasing the Be and Bi values. This can be owed to the decreasing of the effective conductivity in response to increasing Be or Bi values $(\sigma/((1+\mathrm{BeBi})^2+\mathrm{Be}^2))$. Furthermore, the Be and Bi parameters influences on the particle and fluid temperatures distribution are illustrated in Figs. 10 and 11. These Figures specify the rising value of *Be* or *Bi*, as the temperature of the dust and fluid decrease. A rise of Be or Bi reduces the Joule dissipation which is proportional to $(\sigma/((1+\mathrm{BeBi})^2+\mathrm{Be}^2))$.

Conclusions

On an unsteady Magneto-hydrodynamic flow with mass transfer and heat of a dusty fluid was investigated. Thermal radiation, chemical reaction, ion slip, Hall current, Joule and viscous dissipation, and heat generation are considered in the current study. The mathematical solution of the controlling nonlinear partial differential equations was obtained and solved by the finite difference method.

Numerical findings are demonstrated subjected to different influential variables. The summary of the main outcomes is given below.

- The thermal radiation parameter improved the thermal distribution.
- Elevating the Hall parameter increases the velocity distribution of the fluid and dust main velocities.
- The particle and fluid main velocities increase by increasing the ion slip parameter.
- The concentration decreased with the increasing chemical reaction parameter value.
- The particle/fluid temperatures are inversely influenced by differences in Hall and ion slip parameter.

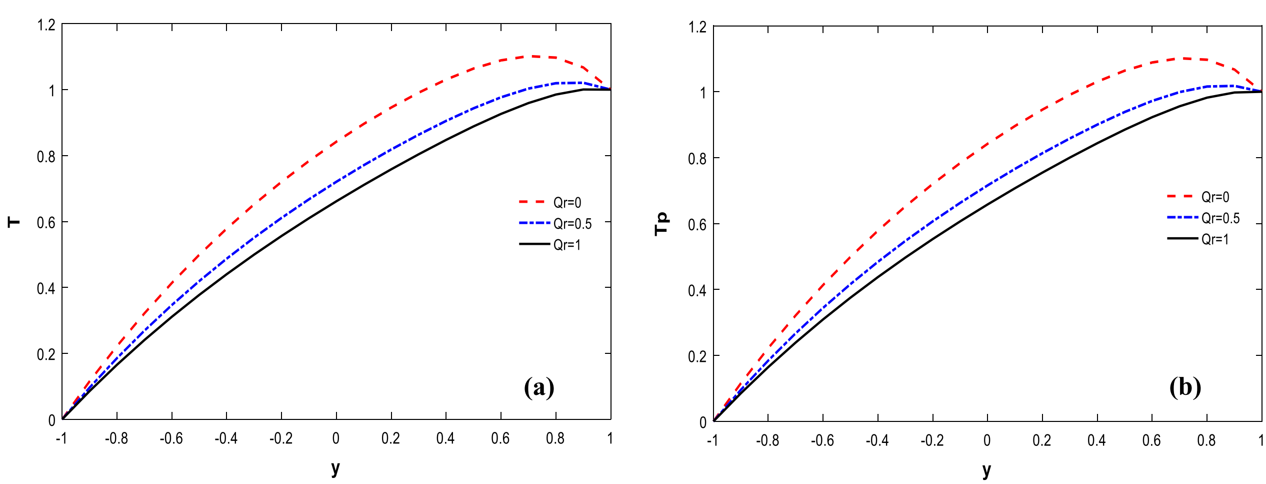

Fig. 6 Influence of Q_r on fluid and particle temperature; **a** T; **b** T_P

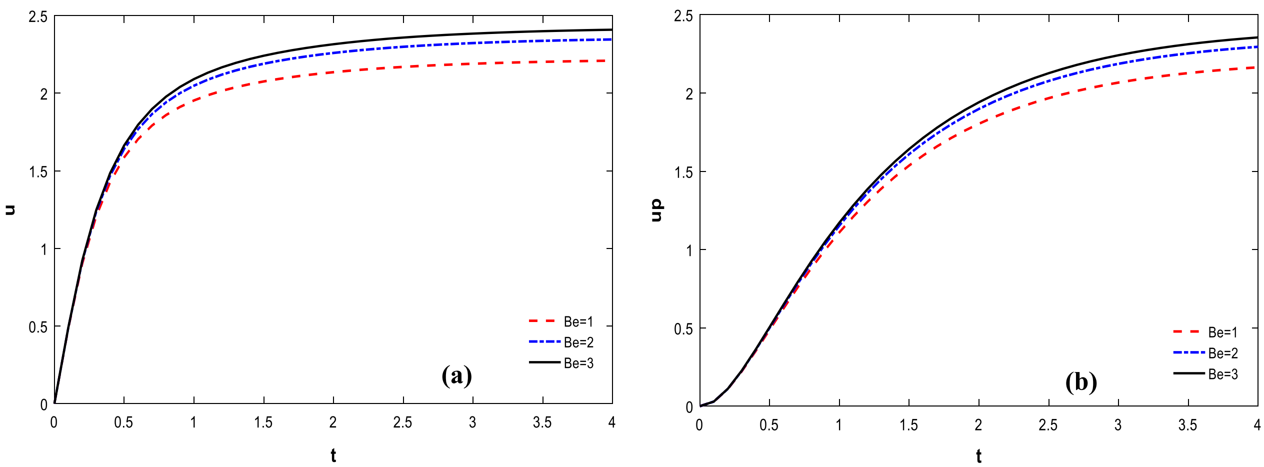

Fig. 8 B_e Influence on the main velocity at channel center; **a** u; **b** u_P

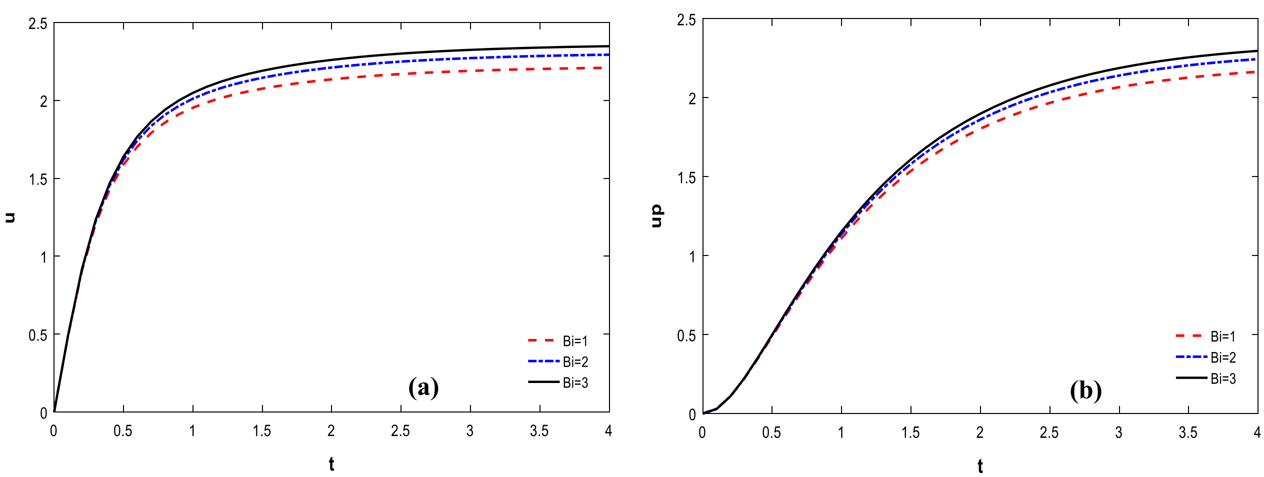

Fig. 9 B_i Influence on the main velocity at channel center; **a** u; **b** u_P

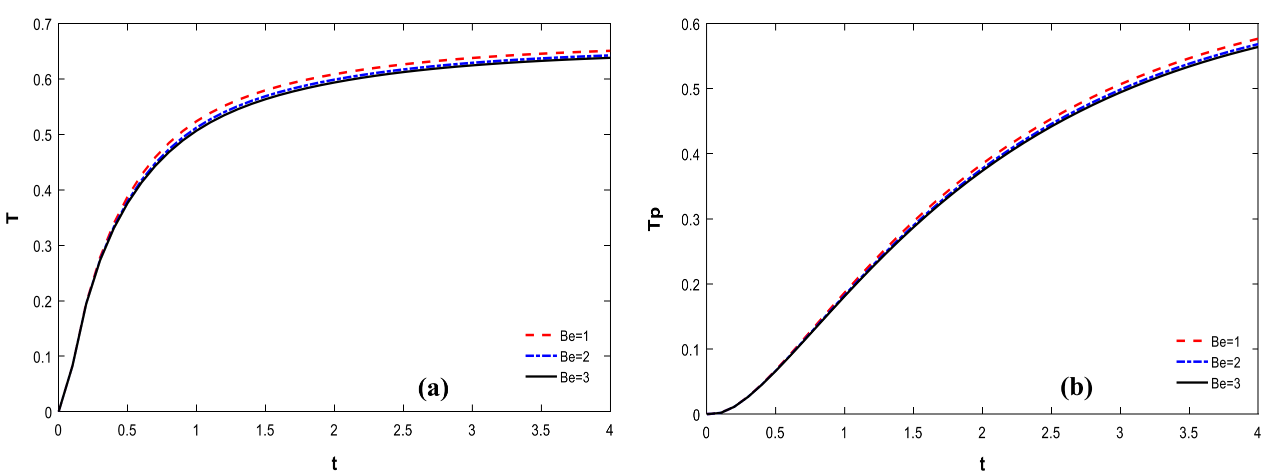

Fig. 10 B_e Influence on fluid and particle temperature at channel center; **a** T; **b** T_P

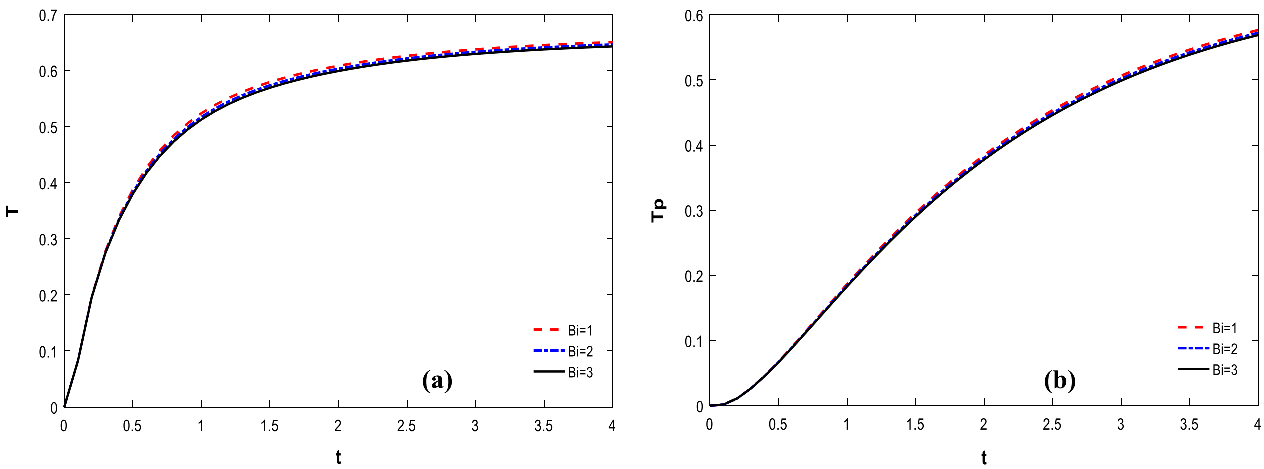

Fig. 11 Influence of B_i on fluid and particle temperature at channel center; **a** T; **b** T_P

Abbreviation

MHD Magnetohydrodynamics

Acknowledgments

Not applicable.

Author contributions

MA team leader who proposed the present paper concept and derived the controlling equations. SB accomplished the analytical solution. OK performed the parametric study. WA performed the numerical solution and MS discussed the results and revised the manuscript. The manuscript was read and agreed by all authors. All authors read and approved the final manuscript.

Funding

Not applicable.

Availability of data and materials

Not applicable.

Declarations

Ethics approval and consent to participate

Not applicable.

Consent for publication

Not applicable.

Competing interests

The authors declare that they have no competing interests.

Received: 6 February 2023 Accepted: 31 March 2023
Published online: 06 April 2023

References

Abbas W, Sayed A (2017) Hall current and joule heating effects on free convection flow of a nanofluid over a vertical cone in presence of thermal radiation. Therm Sci 21:2609–2620

Abbas W, Mekheimer KS, Ghazy MM, Moawad A (2020) Thermal radiation effects on oscillatory squeeze flow with a particle-fluid suspension. Heat Transf 50:2129–2149

Abdeen MAM, Attia HA, Abbas W, Abd El-Meged W (2013) Effectiveness of porosity on transient generalized Couette flow with hall effect and variable properties under exponential decaying pressure gradient. Indian J Phys 87:767–775. https://doi.org/10.1007/s12648-013-0313-5

Abo-zaid OA, Mohamed RA, Hady FM et al (2021) MHD Powell–Eyring dusty nanofluid flow due to stretching surface with heat flux boundary condition. J Egypt Math Soc 29:1–14. https://doi.org/10.1186/s42787-021-00123-w

Attia HA, Abbas W, Abdeen MAM, Emam MS (2014) Effect of porosity on the flow of a dusty fluid between parallel plates with heat transfer and uniform suction and injection. Eur J Environ Civ Eng 18:241–251

Attia HA, Abbas W, Abdin AE-D, Abdeen MAM (2015) Effects of ion slip and hall current on unsteady Couette flow of a dusty fluid through porous media with heat transfer. High Temp 53:891–898

Bafakeeh OT, Raghunath K, Ali F, Khalid M, Tag-Eldin EM, Oreijah MM, Guedri K, Khedher NB, Khan MI (2022) Hall current and Soret effects on unsteady MHD rotating flow of second-grade fluid through porous media under the influences of thermal radiation and chemical reactions. Catalysts 12:1233

Chandrawat RK, Joshi V, Kanchan S (2022) Numerical simulation of interface tracking between two immiscible micropolar and dusty fluids. Mater Today Proc 50:1199–1209. 2nd International conference on functional material, manufacturing and performances (ICFMMP-2021). https://doi.org/10.1016/j.matpr.2021.08.069

Dey D, Chutia B (2020) Dusty nanofluid flow with bioconvection past a vertical stretching surface. J King Saud Univ Eng Sci 34:375–380. https://doi.org/10.1016/j.jksues.2020.11.001

Dey D, Chutia B (2022) Dusty nanofluid flow with bioconvection past a vertical stretching surface. J King Saud Univ Eng Sci 34:375–380. https://doi.org/10.1016/j.jksues.2020.11.001

Ghadikolaei S, Hosseinzadeh K, Ganji D (2018) Numerical study on magnetohydrodynic CNTs-water nanofluids as a micropolar dusty fluid influenced by non-linear thermal radiation and joule heating effect. Powder Technol 340:389–399. https://doi.org/10.1016/j.powtec.2018.09.023

Gireesha B, Mahanthesh B, Thammanna G, Sampathkumar P (2018) Hall effects on dusty nanofluid two-phase transient flow past a stretching sheet using KVL model. J Mol Liq 256:139–147. https://doi.org/10.1016/j.molliq.2018.01.186

Hamid RA, Nazar R, Naganthran K, Pop I (2022) Dusty ferrofluid transport phenomena towards a non-isothermal moving surface with viscous dissipation. Chin J Phys 75:139–151. https://doi.org/10.1016/j.cjph.2021.11.002

Hussein HS (2023) The state of the art of nanomaterials and its applications in energy saving. Bull Natl Res Cent 47:7. https://doi.org/10.1186/s42269-023-00984-4

Islam MR, Ferdows M, Misra JC et al (2022) Two-Dimensional thin layer convective flow and heat transfer of a dusty fluid on a nonlinear stretching sheet. Multiscale Sci Eng 4:111–118. https://doi.org/10.1007/s42493-022-00080-1

Jha BK, Apere CA (2013) Unsteady MHD two-phase couette flow of fluid–particle suspension. Appl Math Model 37:1920–1931. https://doi.org/10.1016/j.apm.2012.04.056
Khan MI, Qayyum S, Hayat T, Waqas M, Khan MI, Alsaedi A (2018) Entropy generation minimization and binary chemical reaction with Arrhenius activation energy in MHD radiative flow of nanomaterial. J Mol Liquids 259:274–283. https://doi.org/10.1016/j.molliq.2018.03.049
Kot MAE, Abbas W (2017) Numerical technique of blood flow through catheterized arteries with overlapping stenosis. Comput Methods Biomech Biomed Eng 20:45–58. https://doi.org/10.1080/10255842.2016.1196198
Kumar D, Satyanarayana B, Kumar R, Kumar S, Deo N (2021) Application of heat source and chemical reaction in mhd blood flow through permeable bifurcated arteries with inclined magnetic field in tumor treatments. Results Appl Math 10:100151. https://doi.org/10.1016/j.rinam.2021.100151
Mahanthesh B, Animasaun I, Rahimi-Gorji M, Alarifi IM (2019) Quadratic convective transport of dusty Casson and dusty Carreau fluids past a stretched surface with nonlinear thermal radiation, convective condition and non-uniform heat source/sink. Phys A Stat Mech Appl 535:122471. https://doi.org/10.1016/j.physa.2019.122471
Mahanthesh B, Shashikumar NS, Gireesha BJ, Animasaun IL (2019b) Effectiveness of hall current and exponential heat source on unsteady heat transport of dusty TiO_2-EO nanoliquid with non- linear radiative heat. J Comput Des Eng 6:551–561. https://doi.org/10.1016/j.jcde.2019.04.005
Mahanthesh B, Mackolil J, Radhika M, Al-Kouz W (2021) Significance of quadratic thermal radiation and quadratic convection on boundary layer two-phase flow of a dusty nano liquid past a vertical plate. Int Commun Heat Mass Transf 120:105029. https://doi.org/10.1016/j.icheatmasstransfer.2020.105029
Meena CS, Kumar A, Roy S, Cannavale A (2022) Review on boiling heat transfer enhancement techniques. Energies 15:5759. https://doi.org/10.3390/en15155759
Michael DH, Miller DA (1966) Plane parallel flow of a dusty gas. Mathematika 13:97–109. https://doi.org/10.1112/S0025579300004289
Mishra S, Sun T-C, Rout B, Ijaz Khan M, Kbiri Alaoui M, Ullah Khan S (2022) Control of dusty nanofluid due to the interaction on dust particles in a conducting medium: numerical investigation. Alex Eng J 61:3341–3349. https://doi.org/10.1016/j.aej.2021.07.026
Muthuraj R, Nirmala K, Srinivas S (2016) Influences of chemical reaction and wall properties on mhd peristaltic transport of a dusty fluid with heat and mass transfer. Alex Eng J 55:597–611. https://doi.org/10.1016/j.aej.2016.01.013
Pandya N, Yadav RK, Shukla AK (2017) Combined effects of Soret–Dufour, radiation and chemical reaction on unsteady MHD flow of dusty fluid over inclined porous plate embedded in porous medium. Int J Adv Appl Math Mech 5:49–58
Peddieson J Jr (1976) Some unsteady parallel flows of particulate suspensions. Flow Turbul Combust 32:239–268
Rafiq M, Sajid M, Alhazmi SE, Khan MI, El-Zahar ER (2022) MHD electroosmotic peristaltic flow of jeffrey nanofluid with slip conditions and chemical reaction. Alex Eng J 61:9977–9992. https://doi.org/10.1016/j.aej.2022.03.035
Saffman PG (1962) On the stability of laminar flow of a dusty gas. J Fluid Mech 13(1):120–128. https://doi.org/10.1017/S0022112062000555
Safwa N, Waini I, Kasim A, Zainal N, Ishak A, Pop I (2022) Magnetohydrodynamic and viscous dissipation effects on radiative heat transfer of non-Newtonian fluid flow past a nonlinearly shrinking sheet: Reiner-Philipp off model. Alex Eng J 61:7605–7617. https://doi.org/10.1016/j.aej.2022.01.014
Tavousi E, Perera N, Flynn D, Hasan R (2023) Heat transfer and fluid flow characteristics of the passive method in double tube heat exchangers: a critical review. Int J Thermofluids 17:100282. https://doi.org/10.1016/j.ijft.2023.100282.100282

Publisher's Note

Springer Nature remains neutral with regard to jurisdictional claims in published maps and institutional affiliations.